Acta Materialia 120 (2016) 273–280

Contents lists available at ScienceDirect

Acta Materialia

journal homepage: www.elsevier.com/locate/actamat

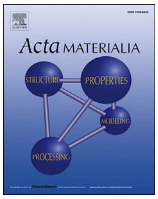

Full length article

Thermoelectric performance of Li doped, p-type $Mg_2(Ge,Sn)$ and comparison with $Mg_2(Si,Sn)$

J. de Boor [a, **, 1], U. Saparamadu [b, 1], J. Mao [b], K. Dahal [b], E. Müller [a, c], Zhifeng Ren [b, *]

[a] *Institute of Materials Research, German Aerospace Center, 51147 Koeln, Germany*
[b] *Department of Physics and Texas Center for Superconductivity, University of Houston, Houston, TX 77204, USA*
[c] *Institute of Inorganic and Analytical Chemistry, Justus Liebig University Giessen, 35392 Giessen, Germany*

ARTICLE INFO

Article history:
Received 31 July 2016
Accepted 22 August 2016

Keywords:
Thermoelectrics
Silicides
Electrical Transport
Mechanical alloying
Electrictronic band structure

ABSTRACT

Solid solutions with chemical formula $Mg_2(Si,Ge,Sn)$ are promising thermoelectric materials with very good properties for the n-type material but significantly worse for the p-type. For power generation applications good n- and p-type materials are required and it has been shown recently that Li doping can enhance the carrier concentration and improve the thermoelectric properties for p-type $Mg_2Si_{1-x}Sn_x$. We have investigated the potential of p-type $Mg_2(Ge,Sn)$ by optimizing $Mg_2Ge_{0.4}Sn_{0.6}$ using Li as dopant. We were able to achieve high carrier concentrations (1.4×10^{20} cm^{-3}) and relatively high hole mobilities resulting in high power factors of 1.7×10^{-3} W m^{-1} K^{-2} at 700 K, the highest value reported so far for this class of material. Exchanging Ge by Si allows for a systematic comparison of $Mg_2(Ge,Sn)$ with $Mg_2(Si,Sn)$ and shows that Si containing samples exhibit a lower power factor but also a lower thermal conductivity resulting in comparable thermoelectric figure-of-merit. The data is furthermore analyzed in the framework of a single parabolic band model to gain insight on the effect of composition on band structure.

1. Introduction

Thermoelectric materials can be used to convert (waste) heat directly into electrical energy. They can thus power autonomous devices or enhance the energy efficiency of various applications and industrial processes [1]. The efficiency of the heat to electrical energy conversion is linked to the thermoelectric figure of merit of the materials, given by $ZT = \sigma S^2/\kappa T$, here σ is the electrical conductivity, κ the thermal conductivity, S the Seebeck coefficient, and T the absolute temperature. A large fraction of the potentially available waste heat can be found in the mid-temperature region between 500 K and 800 K for which several material classes with attractive thermoelectric properties with $ZT > 1$ can be considered, e.g., nanostructured PbTe [2], $CoSb_3$ based skutterudites [3], half Heusler [4], SnSe [5], Cu_2Se based materials [6], and Mg_2Si based solid solutions [7–13]. Among these, Mg_2Si-based solid solutions have the crucial advantage of abundant and non-toxic constituting elements. This makes them one of the most attractive material classes also from an economical point of view [14]. A further material class specific advantage is their low density which is a factor of 2–3 lower than that of skutterudites or PbTe. This holds especially for the binary or Si-rich compositions [15–17] and gives magnesium silicides an advantage where weight is crucial, *i.e.*, in airborne or mobile applications.

Furthermore, magnesium silicides are a technologically relatively advanced material class with systematic contacting studies available [18–22], fabrication and analysis of lab prototypes for thermoelectric modules [23–28] and companies like Alphabet Energy commercializing Mg_2Si-based thermoelectric generators.

However, the excellent thermoelectric properties have been reported only for n-type material, with the p-type being clearly inferior [29,30]. Various dopants have been used to synthesize p-type material [31,32]. Some like Ag are found to be unstable at higher T leading to mixed conduction [33], while others induce holes into the material but far less than expected thus leading to unoptimized material due to too low carrier concentrations. Based on earlier work of Isoda et al. [34], it has been shown recently by Zhang et al. that Li can be employed as an effective dopant in $Mg_2Si_{0.3}Sn_{0.7}$ resulting in carrier concentrations up to

---

[*] Corresponding author.
[**] Corresponding author.
E-mail addresses: Johannes.deboor@dlr.de (J. de Boor), zren@uh.edu (Z. Ren).
[1] Contributed equally.

http://dx.doi.org/10.1016/j.actamat.2016.08.057
1359-6454/

$n \approx 5 \times 10^{20}$ cm^{-3} and a significantly enhanced figure of merit with $ZT_{max} \approx 0.5$ [35]. Tang et al. and Gao et al. furthermore showed that Li can also be employed with $Mg_2Si_{0.4}Sn_{0.6}$ leading to slightly enhanced thermoelectric properties with $ZT_{max} \approx 0.6$ [36,37]. For the n-type material it has been shown that Mg_2(Ge,Sn) has thermoelectric properties comparable to Mg_2(Si,Sn) with the additional advantage that the power factors are systematically larger [38,39]. It is thus the superior material for applications where output power is the main concern, in addition to efficiency. For the p-type material no reports of Mg_2(Ge,Sn) using Li as dopant are available. We have therefore synthesized Li-doped $Mg_2Ge_{0.4}Sn_{0.6}$ using mechanical alloying of the elements. This synthesis technique is well established for the n-type material as it largely avoids Mg-loss and oxidation issues that are often a problem with liquid synthesis techniques [38–40]. We can show that Li is a relatively effective dopant for $Mg_2Ge_{0.4}Sn_{0.6}$ allowing for $n > 10^{20}$ cm^{-3} and $ZT_{max} > 0.5$. We have furthermore synthesized Li-doped $Mg_2Si_{0.4}Sn_{0.6}$ samples using the same synthesis route allowing for a systematic study of the effect of two elements. Further comparison with literature data leads to some understanding of the influence of the (Si/Ge):Sn ratio on thermoelectric properties, band structure and dopant solubility.

2. Experimental

The desired elements Magnesium turning (Mg, 99.98%; Alfa Aesar), tin shots and powder (Sn, 99.8%; Alfa Aesar), germanium pieces (Ge, 99.9999%; Alfa Aesar), silicon granule (Si, 99.999%; Alfa Aesar), and Li shots (99.9%, Alfa Aesar) were loaded into a stainless steel jar in a glove box according to the desired composition and a total mass of 10 g. No excess Mg was added. The elements were ball milled in a Spex 8000 high energy ball mill for a total time of 20 h. During the 20 h the jar was usually inspected 3 times to clear macroscopic inhomogeneity that might have formed during ball milling. After 20 h the powder was of bluish appearance and no inhomogeneity was apparent. Cylindrical pellets were compacted using current assisted sintering with a sintering temperature of 1023 K, a holding time of 2 min, a heating rate of 100 K/min and a pressure of 60 MPa. Temperature dependent electrical conductivity and Seebeck coefficient data was obtained using a ZEM-3, while the thermal conductivity was obtained as the product of the thermal diffusivity D measured by a laser flash measurement system (Netzsch, LFA 457), the mass density ρ by Archimedes' principle, and the specific heat c_p by differential scanning calorimetry (Netzsch, DSC 404 C). The experimental results for the specific heat was averaged for all $Mg_2Ge_{0.4}Sn_{0.6}$ samples and the mean values were used to calculate the thermal conductivity $\kappa = D\rho c_p$; the same was done for the $Mg_2Si_{0.4}Sn_{0.6}$ samples. The precision of S and σ is estimated to be 5%, while the absolute error may be larger [41]. For the κ measurement the uncertainty is estimated to 10%. Hall coefficients were measured at room temperature using a PPMS (Quantum Design, PPMS Dynacool) and a single carrier type was assumed for calculation of carrier density and carrier mobility. X-ray diffraction (XRD) data was obtained using a Siemens D5000 and Rietveld refinement of the lattice parameters a was performed using Topas 4.2. SEM images were taken using a Zeiss Ultra 55 equipped with an energy dispersive X-ray (EDX) detector.

3. Results

A list of samples with nominal compositions and room temperature transport properties is given in Table 1.

The room temperature Hall data shows an increase in charge carrier concentration with increasing Li content x both for the $Mg_2Ge_{0.4}Sn_{0.6}$ and $Mg_2Si_{0.4}Sn_{0.6}$ samples for small x and saturation for $x \geq 0.03$. The Hall mobility μ_H decreases with increasing x.

Exemplary data from powder XRD is presented in Fig. 1. The main peaks correspond to the cubic anti-fluorite structure of Mg_2Si, Mg_2Ge, and Mg_2Sn. The lattice parameter is a=6.611 Å ± 0.002 Å for all $Mg_2Ge_{0.4}Sn_{0.6}$ samples. Most of the spectra also exhibit small peaks that can be identified as elemental Sn. If the Li is not incorporated completely into the lattice but can be found e.g., at the grain boundaries or if some Mg is lost during synthesis the matrix material will be Mg deficient. This can be compensated by segregation of Sn, leading to the observed secondary phase peaks in the XRD data. As Mg_2Sn is less stable than Mg_2Si or Mg_2Ge [42,43] it is plausible that elemental Sn segregates rather than Si or Ge. The results for the $Mg_2Si_{0.4}Sn_{0.6}$ samples are comparable. The theoretical density can be estimated from the refined lattice parameter and all samples listed in Table 1 have a relative density >97%, with most samples >98%.

An SEM picture of the sample with $x = 0.03$ is shown in Fig. 2. Besides the main phase in gray some bright and black spots are visible. The latter ones correspond to the little porosity of the material while the bright spots are possibly due to remains from the polishing process or due to Sn precipitates as also identified in the powder X-ray diffraction data.

The grains in the material show a size distribution in the 0.1 μm–1 μm range, with the crystallites possibly being substantially smaller [36,44]. Pointwise EDX shows a small variation in the material composition $Mg_AGe_BSn_C$ (Li has not been detected), with $1.985 < A < 1.996$, $0.358 < B < 0.391$, and $0.613 < C < 0.657$. The brighter grains are slightly Sn rich compared to the darker ones. This co-existence of neighboring phases with similar but distinct compositions has been observed previously for Mg_2Si based solid solutions [45]. However, the differences are very small so that the material will be treated as single phase material for the electronic transport discussion. We also attempted elemental analysis of the bright spots. These show a slight Mg deficiency and some Sn enrichment but the exact composition cannot be resolved due to the limited spatial resolution of the EDX. It is plausible, though, that these spots contain some elemental Sn that has also been identified in the XRD.

The thermoelectric transport data for the $Mg_{2-x}Li_xGe_{0.4}Sn_{0.6}$ samples is presented in Fig. 3. For better visibility error bars are shown for one sample only but are (relatively) the same for all samples. ZT was calculated from the polynomial fits of S, σ, κ that are shown as solid lines. The lattice thermal conductivity κ_{lat} (plus the bipolar contribution) is calculated from $\kappa_{lat} + \kappa_{bi} = \kappa - \kappa_e = \kappa - L\sigma T$, where κ_e is the electronic contribution to the thermal conductivity and L the Lorenz number that was calculated in the framework of a single parabolic band model, see discussion section.

The electrical conductivity decreases with increasing temperature for low T, while at high temperatures a plateau is observed for some samples, especially those with high Li content. The Seebeck coefficient is positive for all samples, indicating p-type conduction. The magnitude increases linearly with temperature for low temperatures, but the slope decreases with increasing T showing a clear maximum for the lowest doped sample. With increasing x, σ increases while S decrease, however for $x \geq 0.03$ the differences between the samples become small. Overall, the trends are as expected for a degenerate semiconductor, with some deviations in the temperature dependence of some of the samples. The thermal conductivity decreases with increasing temperature for all samples and shows a minimum at ≈600 K due to the onset of the bipolar contribution. The result for $\kappa_{lat} + \kappa_{bi}$ shows the onset of the bipolar more pronounced for the low doped samples as is expected. It can also be seen that the higher doped samples show a somewhat lower $\kappa_{lat}+\kappa_{bi}$, however, the effect is small. The highest power factors are obtained for $x = 0.03$, 0.04 and are